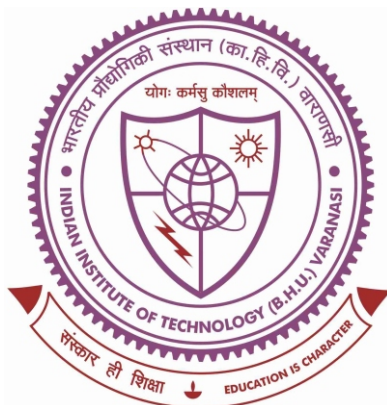


# PVDF Based Polymer-Ceramic Nanocomposites for Capacitive Energy Storage Applications



Thesis submitted in the partial fulfillment for the  
Award of Degree

**Doctor of Philosophy**

By

*Ankit Dwivedi*

SCHOOL OF MATERIALS SCIENCE & TECHNOLOGY  
INDIAN INSTITUTE OF TECHNOLOGY  
(BANARAS HINDU UNIVERSITY)  
VARANASI - 221005  
INDIA

**Roll No. 16111002**

**Year 2024**

*Dedicated*  
*To*  
*My beloved Family*



भारतीय  
प्रौद्योगिकी  
संस्थान  
काशी हिन्दू विश्वविद्यालय



INDIAN  
INSTITUTE OF  
TECHNOLOGY  
BANARAS HINDU UNIVERSITY

## CERTIFICATE

It is certified that the work contained in the thesis entitled "*PVDF Based Polymer-Ceramic Nanocomposites for Capacitive Energy Storage Applications*" by "*Ankit Dwivedi*" has been carried out under my supervision and that this work has not been submitted elsewhere for a degree.

It is further certified that the student has fulfilled all the requirements of comprehensive examination, candidacy and SOTA for the award of Ph.D. degree.

Date.....29/2/2024.....

Place: Varanasi

Ak Singh

**Supervisor**

(Prof. Akhilesh Kumar Singh)

School of Materials Science and Technology

Indian Institute of Technology

(Banaras Hindu University)

Varanasi -221005

Professor/आचार्य

School of Materials Science & Technology/पदार्थ विज्ञान एवं प्रौद्योगिकी स्कूल

Indian Institute of Technology/भारतीय प्रौद्योगिकी संस्थान

(Banaras Hindu University), Varanasi/काशी हिन्दू विश्वविद्यालय, वाराणसी

## DECLARATION BY THE CANDIDATE

I, **Ankit Dwivedi**, certify that the work embodied in this Ph.D. thesis is my own bonafide work carried out by me under the supervision of **Prof. Akhilesh Kumar Singh** for a period from **July 2016** to **Feb 2024** at the **School of Materials Science and Technology**, Indian Institute of Technology (Banaras Hindu University), Varanasi. The matter embodied in this Ph.D. thesis has not been submitted for the award of any other degree/diploma. I declare that I have faithfully acknowledged and given credits to the research workers wherever their works have been cited in my work in this thesis. I further declare that I have not wilfully copied any other's work, paragraphs, text, data, results, *etc.*, reported in journals, books, magazines, reports dissertations, thesis, *etc.*, or available at websites and have not included them in this thesis and have not cited as my own work.

Date..29/02/2024

Place: Varanasi

  
(Ankit Dwivedi)

## CERTIFICATE BY THE SUPERVISOR

This is to certify that the above statement made by the candidate is correct to the best of my knowledge.

  
**Supervisor**

(Prof. Akhilesh Kumar Singh)  
School of Materials Science and Technology  
IIT (BHU), Varanasi  
Professor/आचार्य

School of Materials Science & Technology/पदार्थ विज्ञान एवं प्रायोगिकी स्कूल  
Indian Institute of Technology/भारतीय प्रायोगिकी संस्थान  
(Banaras Hindu University), Varanasi/काशी हिन्दू विश्वविद्यालय, वाराणसी

  
**Coordinator**

School of Materials Science  
& Technology  
IIT (BHU), Varanasi

Coordinator/समन्वयक  
School of Materials Science & Technology/पदार्थ विज्ञान एवं प्रायोगिकी स्कूल  
Indian Institute of Technology/भारतीय प्रायोगिकी संस्थान  
(Banaras Hindu University), Varanasi/काशी हिन्दू विश्वविद्यालय, वाराणसी

## COPYRIGHT TRANSFER CERTIFICATE

**Title of the Thesis:** "PVDF based Polymer-Ceramic Nanocomposites for Capacitive Energy Storage Applications"

**Candidate's Name:** Ankit Dwivedi

### Copyright Transfer

The undersigned hereby assigns to the Indian Institute of Technology (Banaras Hindu University), Varanasi all rights under copyright that may exist in and for the above thesis submitted for the award of the **Ph.D. degree**.

Date: 29/02/2024

Place: Varanasi

Ankit  
(Ankit Dwivedi)

**Note:** However, the author may reproduce or authorize others to reproduce materials extracted verbatim from the thesis or derivative of the thesis for author's personal use provided that the source and the Institute's copyright notice are indicated.

## **ACKNOWLEDGEMENTS**

---

*First of all, I would like to express my deep sense of gratitude to my supervisor **Prof. Akhilesh Kumar Singh**, Coordinator, School of Materials Science and Technology IIT(BHU), Varanasi for his continuous support, guidance, suggestions, encouragement during my Ph.D. research work. His passion, patient, motivation and novel behaviour made me able to continue my Ph.D. research work during my professional undertakings. Further, I would like to thank my ex. Co-Supervisor **Dr. Akansha Dwivedi**, former Assistant Professor, Department of Ceramic Engineering, IIT(BHU) for her continuous support and guidance during initial phase of my Ph.D. journey.*

*I would also like to thanks the faculty members of the school of Materials Science and Technology, Prof. Dhananjai Pandey, Prof. Rajiv Prakash, Prof. Pralay Maiti, Dr. (Mrs.) Chandana Rath, Dr. Chandan Upadhyay, Dr. Bhola Nath Pal, Dr. Ashish Kumar Mishra, Dr. Shrawan Kumar Mishra (Internal RPEC Member), Dr. Sanjay Singh and Dr. Nikhil Kumar, Dr. Ravi Panwar for their suggestions and supports during my Ph.D. work. I would like to thank my external RPEC member Dr. Imteyaz Ahmed, Assistant Professor, Department of Ceramic Engineering, IIT(BHU) for their suggestions, encouragement and guidance. I am also thankful to the faculty members of the Department of ceramic engineering, Prof. Devendra Kumar, Prof. V. K. Singh and Dr. Preetam Singh for their support during experimental work of my Ph.D. thesis.*

*I would like to thank Dr. J. C. Pandey, Assistant Professor, Department of Electrical Engineering IIT (BHU) and Dr. Tanmoy Maiti, Associate Professor, Department of Materials Science and Engineering, IIT Kanpur for their support and encouragement.*

*I heartily acknowledge to Central Instrumental Facility (CIF), IIT (BHU) Varanasi for providing experimental facilities like X-ray diffractometer (XRD), Thermal Gravimetric analysis (TGA), Differential Scanning Calorimetry (DSC), X-ray photoelectron spectroscopy (XPS) and Field Emission Scanning Electron Microscopy (FESEM) and their respective operators during my Ph.D. research work.*

*I would like to express my heartfelt thanks to my lab seniors, Dr. Narendra Kumar Verma, Dr. Dinesh Kumar, Dr. Chandrabhal Singh, Dr. Sushil Kumar, Dr. Monika Singh and Dr. Vijeta Pal for their continuous support and encouragement. I am also thankful to my friends Mr. Krishnakant Dubey, Mr. Abhishek Tripathi, Dr. Shyam Babu, Dr. Pragyanand Prajapati and Dr. Anupam Kumar Singh for their moral support and suggestions. I also would like to thank my juniors Dr. Krishna Prajapati, Ms. Pooja Sonkar,*

*Dr. Vishwa Pratap Singh, Mr. Satyendra Satyarthi, Ms. Srishti Paliwal, Ms. Deepmala, Mr. Prosun Mondal, Ms. Sadhana Yadav, Mr. Deepankar Sri Gyan, Mr. Avinash Pandey and Ms. Sunita Uday for their support and cooperation during experimental work.*

*I express my indebtedness to my parents (Shri Vijay Prakash Dwivedi and Smt. Damyanti Dwivedi) for their trust, love, support and patience to bear my long absence from home during my study. I would like to express my sincere gratitude to my father-in-law Shri Dinesh Kumar Dubey for his trust, love and blessings. I would like to express my heartfelt appreciation to my life partner Mrs. Anshika Dwivedi for her emotional support, love, sacrifice and patience during my Ph.D. research work.*

*I am thankful to all nonteaching staff of the School of Materials Science and Technology, IIT (BHU) for their cooperation at every level. I am also thankful to all who help me directly or indirectly during my research work and they could not be mentioned here.*

*I would like to salute **Mahamana Pandit Madan Mohan Malaviya Ji** for establishing the Capital of Knowledge (Banaras Hindu University) with whom I got the opportunity to study from Graduation to Doctor of Philosophy.*

*I acknowledge Department of Science and Technology (DST), India and IIT (BHU) for financial support as Junior Research Fellow (JRF) and Senior Research Fellow (SRF) to complete Ph.D. research work.*

*Finally, I am grateful to the Almighty God Lord Shiva and Shri Kashi Vishwanath Dham for giving me patience and strength to face all the challenges during Ph.D. journey.*

*(Ankit Dwivedi)*

<b>CONTENTS</b>		<b>Page No.</b>
<b>LIST OF FIGURES.....</b>		xvii
<b>LIST OF TABLES.....</b>		xxiii
<b>LIST OF SYMBOLS &amp; ABBREVIATIONS.....</b>		xxv
<b>PREFACE.....</b>		xxvii
<b>Chapter-I</b>	<b>Introduction and Literature Review .....</b>	<b>1-54</b>
1.1	Introduction.....	1
1.2	Ceramics in perovskite structure.....	3
1.3	Fundamentals of dielectric capacitor.....	5
1.4	Frequency dependent electric polarization.....	13
1.5	Different types of Energy storage dielectric materials.....	14
1.5.1	Linear Dielectrics.....	14
1.5.2	Nonlinear Dielectrics.....	15
1.6	Ferroelectricity in PVDF polymer.....	18
1.7	Dielectric breakdown strength of dielectric material.....	20
1.8	Methods for determination of energy storage density in dielectric Capacitor.....	22
1.9	Interface effect in Polymer nanocomposites.....	25
1.10	Methods to improve the energy storage property of nonlinear dielectric polymers.....	27
1.10.1	Modification of defects.....	28
1.10.2	Blending polymers.....	28
1.10.3	Grafting Polymers.....	29
1.10.4	Polymer based nanocomposites.....	30
1.10.4.1	Polymer based nanocomposites with conducting nanofiller.....	31
1.10.4.2	Polymer based nanocomposites with nonconducting filler.....	37
1.11	Challenges in enhancing the energy storage capacity of polymer-ceramic nanocomposites.....	42
1.12	Effects of Surface Modification of Nanofillers in polymer Nanocomposites.....	45
1.13	Application of PVDF based nanocomposite film.....	51
1.14	Motivation of the thesis.....	53

1.15	Objectives of the present research work.....	53
<b>Chapter-II</b>	<b>Experimental Methods and Characterization Techniques.....</b>	<b>55-83</b>
2.1	Introduction.....	55
2.2	Materials.....	56
2.2.1	Materials used for BST/PVDF composites.....	56
2.2.2	Materials used for BZ/PVDF composite films.....	56
2.2.3	Materials used for BZT/PVDF composite films.....	56
2.3	Synthesis Methods.....	57
2.3.1	Synthesis of nanofiller.....	57
2.3.1.1	Sol gel combustion technique.....	57
2.3.1.2	High Energy ball milling process.....	58
2.3.2	Hydroxylation process of nanoparticles.....	60
2.3.3	Synthesis of PVDF based polymer nanocomposites.....	60
2.3.3.1	Cold Sintering technique.....	61
2.3.3.2	Solution Casting Method.....	63
2.4	Characterization techniques.....	64
2.4.1	X-ray diffraction (XRD) pattern.....	64
2.4.2	Fourier transform infrared spectroscopy (FTIR).....	66
2.4.3	Thermogravimetric Analysis (TGA).....	68
2.4.4	Differential Scanning Calorimetry (DSC).....	70
2.4.5	Field Emission Scanning Electron Microscopy (FESEM).....	71
2.4.6	Impedance Spectroscopy.....	73
2.4.7	P-E hysteresis loop Analysis.....	75
2.4.8	Breakdown strength test set up.....	76
2.4.9	Atomic Force Microscopy.....	79
2.4.10	X-ray Photoelectron Spectroscopy.....	81
2.5	Conclusion.....	83
<b>Chapter-III</b>	<b>Energy Storage Properties of Cold Sintered Ba<sub>0.7</sub>Sr<sub>0.3</sub>TiO<sub>3</sub>/PVDF Polymer Ceramic Nanocomposites.....</b>	<b>85-107</b>
3.1	Introduction.....	85
3.2	Synthesis of Ba <sub>0.7</sub> Sr <sub>0.3</sub> TiO <sub>3</sub> /PVDF nanocomposites.....	88
3.3	Results and discussion.....	90

3.3.1	Structural Analysis.....	90
3.3.2	Density Measurement.....	92
3.3.3	Thermal Analysis.....	94
3.3.4	Microstructural Analysis.....	95
3.3.5	Dielectric Measurement.....	96
3.3.6	P-E hysteresis Analysis.....	101
3.3.7	Weibull Analysis.....	104
3.4	Conclusion.....	106
<b>Chapter IV</b>	<b>BaZrO<sub>3</sub> /Poly (Vinylidene difluoride) Ceramic Nanocomposite Films with Improved Dielectric and Energy Storage Properties.....</b>	<b>109-132</b>
4.1	Introduction.....	109
4.2	Synthesis of BZ/PVDF composite film.....	110
4.3	Results and discussion.....	113
4.3.1	X-ray Diffraction Analysis.....	114
4.3.2	FTIR Analysis.....	115
4.3.3	Thermal analysis using TGA and DSC.....	116
4.3.4	Microstructural Analysis.....	118
4.3.5	X-ray photoelectron spectroscopy Analysis.....	120
4.3.6	Atomic Force Microscopy Analysis.....	122
4.3.7	Dielectric properties.....	124
4.3.8	P-E hysteresis loop Analysis.....	127
4.3.9	Weibull Analysis.....	130
4.4	Conclusion.....	132
<b>Chapter V</b>	<b>BaZr<sub>0.4</sub>Ti<sub>0.6</sub>O<sub>3</sub>/Poly (Vinylidene fluoride) Composite Films with Improved Dielectric and Energy Storage Properties.....</b>	<b>133-154</b>
5.1	Introduction.....	133
5.2	Synthesis of BZT/PVDF composite film.....	135
5.3	Results and Discussion.....	138
5.3.1	X-ray Diffraction Analysis.....	139
5.3.2	FTIR Analysis.....	140
5.3.3	Thermal analysis using TGA and DSC.....	141

5.3.4	Microstructural Analysis.....	143
5.3.5	Atomic Force Microscopy Analysis.....	145
5.3.6	Dielectric properties.....	147
5.3.7	P-E hysteresis loop analysis.....	150
5.3.8	Study of breakdown strength using Weibull Analysis.....	151
5.4	Conclusion.....	153
<b>Chapter-VI</b>	<b>Summary and Future Scope .....</b>	<b>155-160</b>
6.1	Summary.....	155
6.2	Future scope.....	158
<b>References.....</b>		<b>161-181</b>
<b>List of Publications.....</b>		<b>183</b>
<b>List of Conferences/Workshops Attended.....</b>		<b>185-186</b>

## LIST OF FIGURES

<b>Figure No.</b>	<b>Captions</b>	<b>Page No.</b>
Fig. 1.1	Ragone plot representing energy density and power density of dielectric capacitors, Electrochemical supercapacitors and batteries	3
Fig. 1.2	Unit cell of Perovskite structure with general formula $ABO_3$	4
Fig. 1.3	Alignment of permanent dipoles under various conditions: (A) without an external electric field, (B) when subjected to an electric field without molecular interaction, (C) when exposed to an electric field with molecular interaction	8
Fig. 1.4	Electronic polarization of an atom in presence of electric field	11
Fig. 1.5	Ionic Polarization in presence of electric field	11
Fig. 1.6	Orientalional Polarization under the influence of an electric field	12
Fig. 1.7	Interfacial polarization in a dielectric material	13
Fig. 1.8	Frequency dependence of permittivity due to various polarization	14
Fig. 1.9	Frequency dependence of polarizability representing contribution of various polarization mechanisms	14
Fig. 1.10	P-E characteristics of (a) linear dielectrics, (b) paraelectric, (c) ferroelectric, (d) relaxor ferroelectric and (e) antiferroelectric materials	17
Fig. 1.11	Chemical structure of $\alpha$ , $\beta$ and $\gamma$ phase of PVDF	20
Fig. 1.12	Typical dependence of Polarization of Electric field for ferroelectrics in first quarter	24
Fig. 1.13	(a) The polymer matrix with mobile ions, generating a diffuse electrical double layer due to the presence of positively charged particles, resulting electrical potential distribution $\psi(r)$ , (b) Conduction within the composite through the diffuse double layer	26
Fig. 1.14	Representation of Tanaka's model for nanoparticle-polymer interfaces	27
Fig. 1.15	Representation of Blending and grafting process	30

Fig. 1.16	Variation of dielectric permittivity of BT/PVDF composites with BT particle size at different frequencies	38
Fig. 1.17	Variation of permittivity with frequency at different nanofiller loading (a) BSYT/PVDF, (b) PVDF/BT NPs	39
Fig. 1.18	(a) and (b) Variation of dielectric constant and dielectric loss with frequency in case of BST-VC <sub>91</sub> nanocomposite films, (c) and (d) dielectric constant and dielectric loss with BST filler variation	41
Fig. 1.19	(a) Dielectric constant and (b) dielectric loss of NaNbO <sub>3</sub> /PVDF composite and NaNbO <sub>3</sub> /PVDF annealed composite at 1KHz frequency	42
Fig. 1.20	Frequency dependent dielectric constant and dielectric loss of (a) and (c) P(VDF-HFP)/BT@MEEAA NPs, (b) and (d) P(VDF-HFP)/BT NPs	47
Fig. 1.21	(a) Schematic representation depicting the hydroxylation of BaTiO <sub>3</sub> nanoparticles and the establishment of hydrogen bonds in hy-BaTiO <sub>3</sub> /PVDF composites, (b) Illustration outlining the in-situ atom transfer radical polymerization process of MMA monomer initiated from the surface of BaTiO <sub>3</sub> nanoparticles	49
Fig. 1.22	Variation of (a) dielectric permittivity and (b) loss tangent with frequency for BaTiO <sub>3</sub> /PMMA nanocomposites.	50
Fig. 1.23	(a) XRD analysis, (b) FTIR spectra, (c) variation of dielectric constant and dielectric loss with frequency, (d) D-E hysteresis curve, (e) variation of energy storage density with filler content	51
Fig. 2.1	(a) Image of High energy ball milling instrument, (b) Mechanism of high energy ball mill instrument	60
Fig. 2.2	Schematic representation of Cold sintering and Annealing process in case of BaTiO <sub>3</sub> nanocrystalline ceramic synthesis	63
Fig. 2.3	(a) Bragg's law for X-Ray diffraction, (b) Image of the XRD instrument	66
Fig. 2.4	(a) Mechanism of FTIR, (b) Image of FTIR instrument	68
Fig. 2.5	(a) Representation of TGA curve, (b) Image of TGA instrument	70
Fig. 2.6	(a) Representation of DSC curve, (b) Image of DSC instrument	71

Fig. 2.7	(a) Interaction of electron beam with sample in FESEM, (b) Image of FESEM instrument	73
Fig. 2.8	(a) Basic circuit diagram of Impedance spectroscopy, (b) Image of instrument for dielectric property measurement	74
Fig. 2.9	(a) Sawyer-Tower circuit for ferroelectric polarization measurement, (b) Image of PE hysteresis loop analysis instrument	76
Fig. 2.10	(a) Circuit diagram for dielectric breakdown measurement process, (b) Image of breakdown strength test setup	78
Fig. 2.11	(a) Block diagram of AFM instrument, (b) Image of AFM instrument	80
Fig. 2.12	(a) Block diagram of XPS instrument, (b) Image of XPS instrument	83
Fig. 3.1	Schematics for synthesis of BST via Sol- gel combustion process	89
Fig. 3.2	Flow chart describing BST/PVDF composite using cold sintering process	90
Fig. 3.3	(a) XRD pattern of BST sintered ceramic, BST/PVDF composite and BST/PVDF annealed composites, (b) PVDF powder, PVDF hot pressed and PVDF hot pressed annealed at 300 °C.	91
Fig. 3.4	TGA and DSC curve of BST/PVDF composite	94
Fig. 3.5	FESEM image of (a) Conventionally sintered BST ceramic (surface), (b) BST/ PVDF Composite, (c) BST/PVDF composite annealed at 300 °C for 1 hr.	95
Fig. 3.6	Elemental mapping of hot-pressed BST/PVDF composite.	96
Fig. 3.7	(a) Dielectric constant, (b) Loss tangent of BST sintered ceramic and (c) Dielectric constant, (d) Loss tangent of PVDF hot pressed	98
Fig. 3.8	Temperature dependence of dielectric constant of (a) BST/PVDF composite, (c) BST/PVDF annealed composite and Loss tangent of (b) BST/PVDF composite, (d) BST/PVDF annealed composite	100

Fig. 3.9	P-E loop for (a) sintered BST ceramic, (b) BST/PVDF composite (c) BST/PVDF composite annealed at 300 °C for 1 hr.	102
Fig. 3.10	Partial PE hysteresis loop response for Calculation of Energy density and discharge efficiency of pure BST ceramic	103
Fig. 3.11	Partial PE hysteresis loop response for Calculation of Energy density and discharge efficiency of BST/PVDF composite	103
Fig. 3.12	Partial PE hysteresis loop response for Calculation of Energy density and discharge efficiency of BST/PVDF annealed composite	104
Fig. 3.13	Energy density and discharge efficiency for BST ceramic, hot pressed BST/PVDF composite and BST/PVDF annealed composite	104
Fig. 3.14	Weibull plots of dielectric breakdown strength of BST/PVDF annealed composite.	106
Fig. 4.1	Flowchart for Synthesis of BZ particles using High Energy Ball Mill process	112
Fig. 4.2	Synthesis process of BZ/PVDF and hy-BZ/PVDF composite using solution casting method	113
Fig. 4.3	XRD pattern of Pure PVDF film, BZ/PVDF and hy-BZ/PVDF composite film	114
Fig. 4.4	FTIR spectra of (a) hydroxylated BZ powder, (b) pure PVDF, BZ/PVDF and hy-BZ/PVDF composite	116
Fig. 4.5	TGA curve of pure PVDF, BZ/PVDF and hy-BZ/PVDF composite	117
Fig. 4.6	DSC curve of pure PVDF, BZ/PVDF and hy-BZ/PVDF composite	118
Fig. 4.7	FESEM image of (a) hy-BZ powder, (b) PVDF film, (c) BZ/PVDF film, (d) hy-BZ/PVDF composite film, (e-i) Elemental mapping of hy-BZ/PVDF composite film	119
Fig. 4.8	(a-h) X-ray Photoelectron spectra of BZ/PVDF film and hy-BZ/PVDF film	121

Fig. 4.9	(a) AFM micrograph (5x5 $\mu\text{m}$ ) of Pure PVDF film, (b) 3D AFM micrographs (5x5 $\mu\text{m}$ ) of Pure PVDF, (c) AFM micrograph (5x5 $\mu\text{m}$ ) of BZ/PVDF film, (d) 3D AFM micrographs (5x5 $\mu\text{m}$ ) of BZ/PVDF film, (e) AFM micrograph (5x5 $\mu\text{m}$ ) of hy-BZ/PVDF film, (f) 3D AFM micrographs (5x5 $\mu\text{m}$ ) of hy-BZ/PVDF film	123
Fig. 4.10	Roughness profile of (a) Pure PVDF film, (b) BZ/PVDF, (c) hy-BZ/PVDF film	124
Fig. 4.11	Temperature dependance of dielectric constant and dielectric loss (a),(b) for pure PVDF, BZ/PVDF and hy-BZ/PVDF composites, and at different frequencies for (c),(d) BZ/PVDF composite and (e), (f) hy-BZ/PVDF composite	126
Fig. 4.12	PE hysteresis loop for pure PVDF film, BZ/PVDF and hy-BZ/PVDF composite	127
Fig. 4.13	Partial PE hysteresis loop response for calculation of energy density for PVDF film	128
Fig. 4.14	Partial PE hysteresis loop response for calculation of energy density for BZ/PVDF film	129
Fig. 4.15	Partial PE hysteresis loop response for calculation of energy density for hy-BZ/PVDF film	129
Fig. 4.16	Weibull analysis for PVDF film, BZ/PVDF and hy-BZ/PVDF composite film	131
Fig. 5.1	Flow chart for synthesis of BZT powder using high energy ball mill	137
Fig. 5.2	Synthesis process of BZT/PVDF and hy-BZT/PVDF powders using solution casting method	138
Fig. 5.3	XRD pattern of Pure PVDF film, BZT/PVDF and hy-BZT/PVDF composites	139
Fig. 5.4	FTIR spectra of (a) hydroxylated BZT powder, (b) pure PVDF, BZT/PVDF and hy-BZT/PVDF composite	141
Fig. 5.5	TGA curve of pure PVDF, BZT/PVDF and hy-BZT/PVDF composite	142
Fig. 5.6	DSC curve of pure PVDF, BZT/PVDF and hy-BZT/PVDF composite	143

Fig. 5.7	FESEM image of (a) hy-BZT powder, (b) PVDF film, (c) BZT/PVDF film, (d) hy-BZT/PVDF composite film	143
Fig. 5.8	Elemental mapping of hy-BZT/PVDF composite film	144
Fig. 5.9	(a) AFM micrograph (5x5 $\mu\text{m}$ ) of Pure PVDF film, (b) 3D AFM micrographs (5x5 $\mu\text{m}$ ) of Pure PVDF, (c) AFM micrograph (5x5 $\mu\text{m}$ ) of BZT/PVDF film, (d) 3D AFM micrographs (5x5 $\mu\text{m}$ ) of BZT/PVDF film, (e) AFM micrograph (5x5 $\mu\text{m}$ ) of hy-BZT/PVDF film, (f) 3D AFM micrographs (5x5 $\mu\text{m}$ ) of hy-BZT/PVDF film	146
Fig. 5.10	Roughness profile of (a) Pure PVDF film, (b) BZT/PVDF, (c) hy-BZT/PVDF film	147
Fig. 5.11	Variation of dielectric constant and dielectric loss with temperature (a),(b) for pure PVDF, BZT/PVDF and hy-BZT/PVDF composites, and at different frequencies for (c),(d) BZT/PVDF composite and (e), (f) hy-BZT/PVDF composite	149
Fig. 5.12	PE hysteresis loop for pure PVDF, BZT/PVDF and hy-BZT/PVDF composite	151
Fig. 5.13	Weibull analysis for pure PVDF film, BZT/PVDF composite and hy-BZT/PVDF composite film	153

## LIST OF TABLES

<b>Table No.</b>	<b>Caption</b>	<b>Page No.</b>
Table 3.1	Bulk densities of sintered BST ceramic, BST/PVDF composite and BST/PVDF annealed composite.	93
Table 3.2	A comparison of the dielectric permittivity of different BST/Polymer Composites.	100
Table 3.3	Remnant Polarization ( $P_r$ ), Maximum Polarization ( $P_m$ ), Energy storage density ( $U_e$ ) and discharge efficiency ( $\eta$ ) of Pure BST, BST/PVDF composite and BST/PVDF annealed composite.	102
Table 4.1	Remnant Polarization ( $P_r$ ), Maximum Polarization ( $P_m$ ), Energy storage density ( $U_e$ ) and discharge efficiency ( $\eta$ ) of pure PVDF film, BZ/PVDF and hy-BZ/PVDF composite film	128
Table 4.2	Comparison of the dielectric permittivity and energy storage density of different reported PVDF based Composites with hy-BZ/PVDF composite film	130
Table 5.1	Remnant Polarization ( $P_r$ ), Maximum Polarization ( $P_m$ ), Energy storage density ( $U_e$ ) and discharge efficiency ( $\eta$ ) of pure PVDF film, BZT/PVDF and hy-BZT/PVDF composite film	151
Table 5.2	Comparison of the dielectric permittivity and energy storage density of different reported PVDF based Composites with hy-BZT/PVDF composite film	153



## List of Symbols & abbreviations

$\eta$	Energy efficiency
$\alpha$	Polarizability
$U$	Energy density
$\text{\AA}$	Angstrom
$\psi$	Electric potential barrier
Hz	Hertz
T	Temperature
$T_c$	Curie temperature
$\chi$	Susceptibility
$\sigma$	Conductivity
$\phi$	Filler volume fraction
$\mu\text{m}$	Micrometer
$\epsilon$	Dielectric Permittivity
P	Polarization
$E_c$	Coercive field
$P_{\text{max}}$	Maximum polarization
$P_s$	Spontaneous polarization
$P_r$	Remnant polarization
$E_b$	Breakdown strength
XPS	X-ray spectroscopy
FESEM	Field emission scanning electron microscopy
FTIR	Fourier transform infrared
XRD	X-Ray diffraction
XPS	X-ray photoelectron spectroscopy
AFM	Atomic force microscopy
PVDF	Polyvinylidene difluoride



## PREFACE

---

The scientific community is focusing on energy storage options due to the current energy crisis and severe air pollution resulting from burning of conventional fossil fuels. There is a significant demand for the research and development of innovative, environmentally friendly energy systems and associated energy storage technologies. Dielectric capacitors show promise as energy storage systems in various applications such as transportation and portable electronic devices, thanks to their high-power density, long lifespan, and extensive cyclic life. However, their energy density is comparatively low as compared to conventional batteries, hindering efforts to further improve these storage devices<sup>1</sup>. Despite this limitation, capacitors have a crucial role in energy storage technologies due to their rapid charging and discharging capabilities, which batteries lack.

Dielectric capacitors typically consist of dielectric materials with excellent storage properties. Ceramic dielectrics exhibit a high dielectric constant, low dielectric loss, and a broader temperature operating range. However, due to the toxic nature of common lead based dielectrics, their use is limited in research. BaTiO<sub>3</sub>-based electro-ceramics present a potential alternative to lead-based dielectrics, offering breakdown strength of 145-450 kV/cm.<sup>2</sup> Over the past few years, many other electro ceramics with comparable dielectric strength and energy density have been developed. However, their lower dielectric breakdown strength limits their application in power electronics.

On other hand, polymers are characterized by lower dielectric constants, high energy storage density, and high dielectric breakdown strength. When compared to dielectric ceramics, the dielectric constant of dielectric polymers is notably lower. Noteworthy examples include Polyvinylidene fluoride (PVDF), Biaxially Oriented Polypropylene (BOPP), and Poly(methyl methacrylate) (PMMA) with reported dielectric

constant values of  $\sim 10$ ,  $\sim 2$ , and  $5$  respectively<sup>2</sup>. To tailor these polymers for energy storage applications, researchers often modify them by synthesizing nanocomposites, using the polymer as a matrix. PVDF, in particular, has drawn significant attention due to its exceptional dielectric properties, prompting extensive research to enhance these properties further. Basically, PVDF based polymer nanocomposites have been synthesized using conducting/semiconducting and nonconducting fillers.

Nanoparticles with semiconducting/conducting properties have been investigated as nanofillers within the PVDF matrix to enhance its dielectric properties. PVDF based composites with conducting/semiconducting filler can exhibit high dielectric permittivity with proper proportion of filler loading. High dielectric permittivity can only be achieved when the filler loading is very close to and less than the percolation threshold. Many synthesized PVDF-based polymer nanocomposites have shown promising outcomes. Such high permittivity values have been reported in various percolative polymer composites with different conductive/semiconducting particles, including metal particles, carbon nanofibers, CNTs, graphene, TiO<sub>2</sub> and ZnO<sup>3-6</sup>. Optimal energy density has been achieved up to a specific vol% of such nanofillers, but excessive filler amounts can cause percolation in nanocomposites, compromising their properties. The nanocomposites transition into behaving partially conducting beyond the percolation threshold, creating numerous conducting paths in composite films. Although polymer nanocomposite with conductive filler have successfully achieved favourable dielectric permittivity and low percolation threshold, they still face ongoing challenges including elevated dielectric loss, diminished dielectric strength, and a limited processing window that significantly hinder their applications in high energy storage application. The incorporation of conductive fillers increases dielectric permittivity in nanocomposites because of Maxwell Wagner Sillars (MWS) polarization or micro capacitor effect, yet it concurrently leads to high dielectric

loss and leakage current via conductive particle network formed near critical percolation threshold, which causes a drastic reduction in breakdown strength<sup>7,8</sup>. One frequently cited explanation for this phenomenon is that the development of micro capacitors results in an unusually expansive local electric field within the pristine polymer region due to the close proximity of adjacent nanoparticles. As the polymer layer between these neighboring particles is excessively thin to withstand the escalating local electric field, it leads to a short circuit, giving rise to a substantial leakage current<sup>7</sup>.

On the other hand, PVDF based nanocomposites using nonconducting/ceramic filler have also been synthesized for energy storage applications. High dielectric constant ceramics, such as BaTiO<sub>3</sub>, lead-based and SrTiO<sub>3</sub>, have been employed as fillers to reinforce in the PVDF matrix<sup>9</sup>. The incorporation of these fillers has resulted in increased dielectric constant and polarization, consequently boosting the energy storage density of the polymer nanocomposites. There appears to be less limitation in the reinforcement of dielectric ceramics in PVDF, with fillers reaching over 50 vol% to achieve the desired energy density and dielectric properties in comparison to PVDF based nanocomposites using conducting filler. For instance, reinforcing 60 vol% BaTiO<sub>3</sub> in the PVDF matrix elevated the dielectric constant from ~9 to ~125, with surface modification of the filler using Polyvinylpyrrolidone (PVP)<sup>2</sup>. Recent research indicates that the energy density of PVDF/BaTiO<sub>3</sub> nanocomposites is optimal at 3 vol% filler loading. Other surfactants like H<sub>2</sub>O<sub>2</sub>, ethylene diamine, -NH<sub>2</sub>, polydopamine (PDOPA) have been successfully used to modify the surface of the nanofillers to get improved dielectric and energy storage properties in various reported literature<sup>1,10</sup>.

In our current research, we have chosen PVDF as polymer for developing nanocomposites with different nonconducting/ceramic BaTiO<sub>3</sub> based ceramics for high-energy storage applications. PVDF can exist in four crystalline phases namely  $\alpha$  as a

nonpolar phase,  $\beta$ ,  $\gamma$  and  $\delta$  as polar phases. By employing suitable processing methods or forming nanocomposites with appropriate ceramics and polymer, the nonpolar phase of PVDF can be converted into electroactive polar phases. Ceramic fillers have been used to enhance the dielectric and energy storage properties of the nanocomposites. Our investigation into these nanocomposites has yielded several noteworthy findings, briefly outlined below.

### **1. Energy storage properties of cold sintered $\text{Ba}_{0.7}\text{Sr}_{0.3}\text{TiO}_3$ /PVDF Polymer Ceramic Nanocomposites**

$\text{Ba}_{0.7}\text{Sr}_{0.3}\text{TiO}_3$ /PVDF (Polyvinylidene fluoride) ceramic-polymer composites have been synthesized using a cold sintering process.  $\text{Ba}_{0.7}\text{Sr}_{0.3}\text{TiO}_3$  (BST) nanoparticles are synthesized using sol-gel combustion method. The BST nanoparticles are used for synthesizing the  $\text{Ba}_{0.7}\text{Sr}_{0.3}\text{TiO}_3$ -PVDF composite with 80wt.% BST and 20 wt. % PVDF. X-ray diffraction analysis confirmed pure phase formation of BST and revealed presence of different phases of PVDF in certain conditions. XRD pattern confirms the formation of pure perovskite phase of BST with cubic structure having Pm-3m space group. In case of BST/PVDF composite, crystallization of  $\beta$  phase and in case of annealed BST/PVDF composite, crystallization of  $\gamma$ -phase dominates. Thermal stability and surface morphology of the composite has been studied using thermo-gravimetric analysis and SEM respectively. TGA/DSC analysis reveals that composite is stable for the application up to 300 °C. Dielectric and ferroelectric properties have been studied. Thermally stable dielectric constant and dielectric loss is obtained from room temperature to 200 °C in case of annealed BST/PVDF composites. Polarization-Electric field hysteresis loop analysis of composite reveals that significantly higher dielectric breakdown strength (more than 400 kV/cm) have been achieved in comparison to pure ceramic which is the main criteria for a potential material for energy storage purpose. Discharge efficiency of BST/PVDF annealed

composite upto 95 % and high thermal stability up to 300 °C has been achieved in case of BST/PVDF annealed composite which is big achievement for a ceramic matrix composite with polymer filler.

## **2. BaZrO<sub>3</sub>/Poly (Vinylidene difluoride) Ceramic Nanocomposite Films with Improved Dielectric and Energy Storage Properties**

BaZrO<sub>3</sub> (BZ)/PVDF (Polyvinylidene difluoride) Polymer nanocomposites have been synthesized for energy storage applications using solution casting method. Barium zirconate (BZ) has been synthesized using high energy ball mill method and BZ/PVDF ceramic nanocomposites have been synthesized in thin film form using 90 wt. % PVDF polymers as a matrix and 10 wt.% BZ as nanofillers. XRD analysis has been performed to check successful synthesis of nanocomposites. We have synthesized pure PVDF film, BZ/PVDF and hydroxylated (hy)-BZ/PVDF composite film and we have achieved value of dielectric constant for the hy-BZ/PVDF composite film ( $\epsilon_r \sim 26$ ) almost three times of the value of dielectric constant for pure PVDF film. FTIR spectra of hy-BZ powder shows the successful hydroxylation of BaZrO<sub>3</sub> filler. TGA curve shows that there is no weight loss observed upto 450<sup>0</sup>C in case of composites. XPS and AFM analysis has also been performed for above synthesized composites. Polarization has been also increased upto almost double in case of hy-BZ/PVDF composite in comparison to pure PVDF film. We have achieved energy storage density of 1.11 J/cm<sup>3</sup> for hy-BZ/PVDF composite much higher than the pure PVDF which is equal to 0.47 J/cm<sup>3</sup>. The dielectric breakdown strength has also been analysed using Weibull analysis technique and obtained 1495 kV/cm in case of hy-BZ/PVDF composites.

### **3. BaZr<sub>0.4</sub>Ti<sub>0.6</sub>O<sub>3</sub>/Poly (Vinylidene fluoride) Composite Films with Improved Dielectric and Energy Storage Properties**

We have synthesized BaZr<sub>0.4</sub>Ti<sub>0.6</sub>O<sub>3</sub> (BZT) ceramic nanoparticles using nano mill process and hydroxylated (hy)-BZT/PVDF composite film using solution casting method with 10 wt. % of BZT nanoparticle as filler and 90 wt. % of PVDF polymer as a matrix. XRD patterns of composites confirm the successful formation of composites. FTIR spectra confirms the successful hydroxylation of BZT powder for better dispersion. Differential scanning calorimetry analysis represents improved degree of crystallinity in case of composites. AFM analysis has also been performed for synthesized composites. The dominance of polar phase of PVDF in composites was observed due to interfacial interaction among filler nanoparticles. The significantly enhanced dielectric permittivity ( $\epsilon_r \sim 25.5$ ) and ferroelectric properties have been obtained in case of hy-BZT/PVDF composite film in comparison to pure PVDF film ( $\epsilon_r \sim 8$ ). The value of dielectric breakdown strength for hy-BZT/PVDF composite has been calculated using Weibull analysis and found to be 1754 kV/cm. We have calculated energy storage density using Weibull analysis for hy-BZT/PVDF composite and was found to be 0.41 J/cm<sup>3</sup> at electric field of 790 kV/cm. The above synthesized composites may be a suitable replacement with improved dielectric properties for energy storage applications.

The thesis is organized into six chapters.

**Chapter-I:** This chapter describes basic introduction about energy storage materials. The basic concepts related to dielectric materials, energy storage in various dielectric materials, energy density and dielectric breakdown strength have been discussed in detail. The brief review of the reported literature on polymer based composite materials using conducting/semiconducting and nonconducting filler for energy storage applications has been discussed. Objective of the present thesis work is discussed in the last of the chapter.

**Chapter-II:** This chapter describes different synthesis methods for ceramic and PVDF based polymer ceramic nanocomposite materials. Cold sintering process and solution casting method for PVDF based polymer ceramic composites have been described in detail. The use of different materials and chemicals has also been discussed. The various characterization techniques used in the study of various synthesized composites have also been discussed in this chapter.

**Chapter-III:** This chapter involves synthesis of PVDF polymer-based nanocomposites using BST ceramic as a matrix and PVDF polymer as a filler with the help of cold sintering technique. Experimental results obtained from synthesized samples have been discussed using various characterization techniques. The dielectric properties, energy storage properties and dielectric breakdown strength have been discussed in detail. Experimental results obtained in this chapter has been published in the **Journal of Materials Science: Materials in Electronics 34 (2023) 1939**.

**Chapter-IV:** In this chapter, we have described synthesis of hy-BaZrO<sub>3</sub>/PVDF nanocomposite films with the help of solution casting process using 90 wt. % PVDF polymer as a matrix and 10 wt.% BZ as nanofiller. We have achieved higher dielectric constant for the hy-BZ/PVDF composite film ( $\epsilon_r \sim 26$ ) almost three times in comparison to pure PVDF film and energy storage density 1.11 J/cm<sup>3</sup> for hy-BZ/PVDF composite much higher than the pure PVDF which is equal to 0.47 J/cm<sup>3</sup>. The dielectric breakdown strength has also been analysed using Weibull analysis technique and found to be 1495 kV/cm in case of hy-BZ/PVDF composites.

**Chapter-V:** Synthesis of PVDF based nanocomposites with reinforced BZT as a filler has been performed and energy storage properties have been studied. Significant improvement in the value of dielectric constant has been obtained in case of hy-BZT/PVDF

nanocomposites in comparison to pure PVDF film. The value of dielectric breakdown strength for hy-BZT/PVDF composite has been calculated using Weibull analysis and found to be 1754 kV/cm.

**Chapter-VI:** This chapter summarizes the outcome of present thesis work and future scope in this area.